(2)

R & D STATUS REPORT

DARPA ORDER NO: 8100 **PROGRAM CODE NO:** DO-C9

CONTRACTOR: David Sarnoff Research Center

CONTRACT NO.: N00014-91-C-0216 **CONTRACT AMOUNT:** $1,585,150

EFFECTIVE DATE OF CONTRACT: 26 August 1991

EXPIRATION DATE OF CONTRACT: 25 August 1994

PRINCIPAL INVESTIGATOR: Dr. Edgar J. Denlinger

TECHNICAL CONTRIBUTORS: Dr. Aly Fathy, David Kalokitis, Valerie Pendrick, Dr. K. S. Harshavardhan (Neocera), Dr. Albert Piqué (Neocera), Dr. Erwin Belohoubek, Dr. T. Venkatesan (Neocera)

TELEPHONE NO: (609) 734-2481

SHORT TITLE OF WORK: High Performance YBCO Films

REPORTING PERIOD: Period 8/1/92 to 10/31/92

1	The views and conclusions contained in this document are those of the authors and should not be interpreted as necessarily representing the official policies, either expressed or implied, of the Defense Advance Research Projects Agency of the U.S. Government.
2	Ownership in Patent Data included herein is retained by the contractor/subcontractor pursuant to FAR 52.227-12.

TABLE OF CONTENTS

DESCRIPTION OF PROGRESS:

SUMMARY

The objective of this program is to identify suitable low loss, low dielectric constant substrates and develop and optimize deposition processes for high quality YBCO films including the necessary buffer layers. Ultimate goals are large area substrates having double-sided HTS coating with a surface resistance ten times lower than copper at 40 GHz. High quality HTS films on low dielectric constant substrates are expected to find widespread use in advanced millimeter wave components, in extending the power handling capability of microwave and millimeter wave circuitry, and in facilitating high speed computer interconnects. Sample demonstration circuits will be built toward the end of the program.

We have successfully deposited a high quality YBCO film on a good low loss and low dielectric constant substrate, magnesium fluoride ($\varepsilon \approx 5$). With the use of two buffer layers (magnesium oxide and strontium titanate) between the YBCO and the substrate, transition temperatures of 89°K and transition widths of about 0.5°K were achieved. The critical current density J_c of 4×10^6 A/cm^2 at 77K in zero field is among the highest reported for YBCO films. The magnesium fluoride (MgF_2) substrate has a tetragonal structure with a dielectric constant of 5.2 in the plane of the substrate and 4.6 perpendicular to the substrate surface. It has a good hardness (~ 575 Knoop) and a linear thermal expansion coefficient that closely matches YBCO and the buffer layers. Dielectrometer measurements on a thin unmetallized 2.5cm square sample of the material resulted in a microwave loss tangent of about 10^{-4} at 77K, which makes the material very useful at both microwave and millimeter wave frequencies. The dielectric resonator test at 24GHz was used for measuring the surface resistance of unpatterned YBCO films on the MgF_2 substrate and gave results that closely matched those achieved with previous YBCO films on lanthanum aluminate. A meander line resonator test for characterizing a patterned YBCO film on the substrate over a 2-14 GHz range yielded unloaded Q's (or effective surface resistance) that were an order of magnitude better than a copper-patterned substrate.

Two types of YBCO on MgF_2 sample circuits for mm-wave operation (35GHz) have been designed: (1) narrow band filters for multiplexers; and (2) power dividers for array antenna feed networks. Modelling efforts have predicted

greater than a 3X improvement in loss over Cu with a single-sided HTS substrate (Au ground plane) and a 10X improvement with a double-sided HTS substrate.

I. HTS MATERIAL DEVELOPMENT

This report summarizes our experimental results on YBCO films deposited on (001) MgF_2 substrates. The main features are

1) Identification of (001) MgF_2 as the substrate among all other alkaline earth fluorides
2) Optimization of (100) MgO as a first buffer on (001) MgF_2
3) Optimization of (100) $SrTiO_3$ as the second buffer layer on (100) MgO
4) Optimization of YBCO film growth

A. Properties of the (001) MgF_2 Substrate

Previously we experimented with YBCO films on (001) oriented SrF_2 substrates due to the desirable cubic crystal structure of this substrate which commensurates with the crystal structure of some of the buffer layers, such as cubic MgO. The choice of MgF_2 as a substrate has been made on account of it's desirable dielectric properties relative to SrF_2. Even though MgF_2 has an *undesirable* tetragonal structure, its ε (5.2 at 77K) is isotropic in the plane of the film and lower than the ε for cubic SrF_2 (6.2 at 77K). Further, MgF_2 is mechanically harder than SrF_2 on which most of the depositions were carried out until now. More material data is provided below.

Magnesium Fluoride (MgF_2) Material Properties

Structure: Tetragonal, a=4.623 Å, c=3.052Å

Melting Point: 1585°K

Boiling Point: 2510°K

Hardness: ~575 (Knoop)

Dielectric Constant: 5.2 ($\perp$ c-axis); 4.6 ($||$c) at 77K

Linear Thermal Expansion Coefficient: (323 - 883K)

$\perp$c: 9.2×10^{-6}/°C

$||$c: 13.3×10^{-6}/°C

The relative Knoops hardness ratings for the alkaline earth fluorides are provided here in Table I, clearly suggesting the superior mechanical properties of the MgF_2 over the other fluorides. For comparison, the Knoop's hardness of MgO is also provided.

Table I.

Material	Knoop's hardness (Kg/mm^2)	ε_r (77 K)
MgF_2	575	5.2 ($\perp$c); 4.6 ($\|\|$c)
SrF_2	130	6.2
CaF_2	120	6.5
BaF_2	65	7.0
MgO	675	9.5

Accordingly, our subsequent work is focused on depositing high quality YBCO films on (001) oriented MgF_2 substrates.

B. Choice of (100) MgO and (100) $SrTiO_3$ Buffer Layers

MgF_2 and the other alkaline earth fluorides are chemically reactive at the high growth temperatures and high oxygen partial pressures are needed to obtain high quality films. Though it is possible to grow YBCO films directly on these substrates at relatively lower temperatures, the superconducting properties of these films are rather poor (with the transition temperatures around 80-83 K) relative to the high quality films grown on substrates like $SrTiO_3$ or $LaAlO_3$ at the higher growth temperatures. Further, it is also observed that even at these lower temperatures direct deposition of the films leads to film-substrate reactions. To obtain high quality YBCO films on these reactive fluoride substrates, the use of suitable buffer layers is therefore mandatory.

In the present study we used two buffer layers. The first one is a (100) oriented MgO layer, deposited on (001) MgF_2 substrates. The second one is a (100) $SrTiO_3$ buffer layer over the (100) MgO buffer layer.

We have used MgO and $SrTiO_3$ as buffer layers due to the following reasons:

1. Due to the chemical reactivity of the MgF_2 substrate at the high growth temperatures and high oxygen partial pressures, it is essential to "passivate" the substrate surface with an epitaxial buffer layer which can be grown at relatively lower temperatures and oxygen partial pressures. (100) MgO is one such possibility.

2. For depositing high quality YBCO films it is essential that the buffer layer provides an epitaxial template to the subsequent growth. $SrTiO_3$, which has the best epitaxial matching with regards to YBCO, would be an ideal choice if it can be grown on the (100) MgO layer.

Conventionally, the two buffer layers, ytrria stabilized zirconia (YSZ) and CeO_2 have been among the most popular, which is mainly due to the success achieved in their use in conjunction with "reactive" substrates such as R-plane sapphire, Si and a variety of other metallic substrates. In the present work we attempted to grow YSZ and CeO_2 buffer layers in the desired (100) orientation over the (001) MgF_2 substrate with little success. The films are often polycrystalline in nature with mixed orientations, and further, due to the high temperatures and high oxygen partial pressures required to promote the (100) orientation, the films also reacted with the underlying MgF_2 substrate. Attempts to deposit at relatively lower temperatures led to poorly formed phases (structurally) as revealed by their x-ray data.

It has recently been suggested [1] that fast diffusion on the neutral cleavage planes of strongly ionic systems can make epitaxial growth possible down to remarkably low temperatures ~ 0.1 T_m, T_m being the melting temperature of the material being grown. These workers have grown single crystalline thin films of (100) MgO on (100) surfaces of MgO substrates at temperatures as low as 140 K. Their explanation is that the corrugated electrostatic potential due to the ions decays exponentially outside a neutral ionic surface to leave only weak barriers impeding the mobility of surface species. Similar considerations prompted us in the present study to look into the possibility of growing (100) MgO on the strongly ionic (001) MgF_2 substrates. We find that the growth of (100) MgO on (001) MgF_2 indeed takes place at relatively lower temperatures and lower oxygen partial pressures, conditions at which the film-substrate reactions are insignificant.

The choice of $SrTiO_3$ as the second buffer layer in the present study has been made on the following accounts. The microstructure of YBCO films grown

on (100) MgO substrates has previously been analyzed. Due to the large lattice mismatch of 8.8% between MgO (a=4.21Å) and YBCO (a=3.82Å, b=3.89Å), the films exhibit a polycrystalline mosaic microstructure. The orientational relationship between the MgO substrate and the YBCO film are established as [110] YBCO ||[100] MgO in the (a-b) plane of the film and [001] YBCO ||[001] MgO along the c-axis of the film. Further, in the resulting mosaic microstructure, the in-plane orientational relationship is different from one grain to another. The absence of a complete a-b plane locking results in a c-axis oriented polycrystalline film in which the grain boundaries act as weak links resulting in microwave losses. On the other hand, YBCO films grown on substrates such as $SrTiO_3$ with a closer lattice match (a=3.9Å) exhibit a single crystalline microstructure with epitaxial relationships such as [100] YBCO ||[100] $SrTiO_3$ in the (a-b) plane of the film and [001] YBCO ||[001] $SrTiO_3$ along the c-axis of the film. We deposited $SrTiO_3$ as a second buffer layer mainly to provide an ideal epitaxial structural template over the (100) MgO buffer layer for the subsequent YBCO film growth. A recent paper [2] also points out significant improvements in the quality of the YBCO film when $SrTiO_3$ is used as a buffer over the (100) MgO substrate.

C. YBCO Film Deposition

In the present study, all the film depositions (the buffer layers as well as YBCO) are carried out using a multi-target carousel in a single pump-down cycle. Fig. 1 shows a typical x-ray diffraction profile of MgO buffer layer which is optimized to grow in the desire (100) orientation over (001) MgF_2. Fig. 2 presents the x-ray pole figure data (ϕ scans) and Fig. 3, the Θ-2Θ date of the substrate-buffer layer-YBCO film combination indicating that the scheme we have employed enables us to obtain high quality YBCO films with a "cube on cube" epitaxial relationships as follows.

[001] MgF_2 || [100] MgO || [100] $SrTiO_3$ || [100] YBCO (in the plane of the film).
[001] MgF_2 || [001] MgO || [001] $SrTiO_3$ || [001} YBCO (along the film normal).

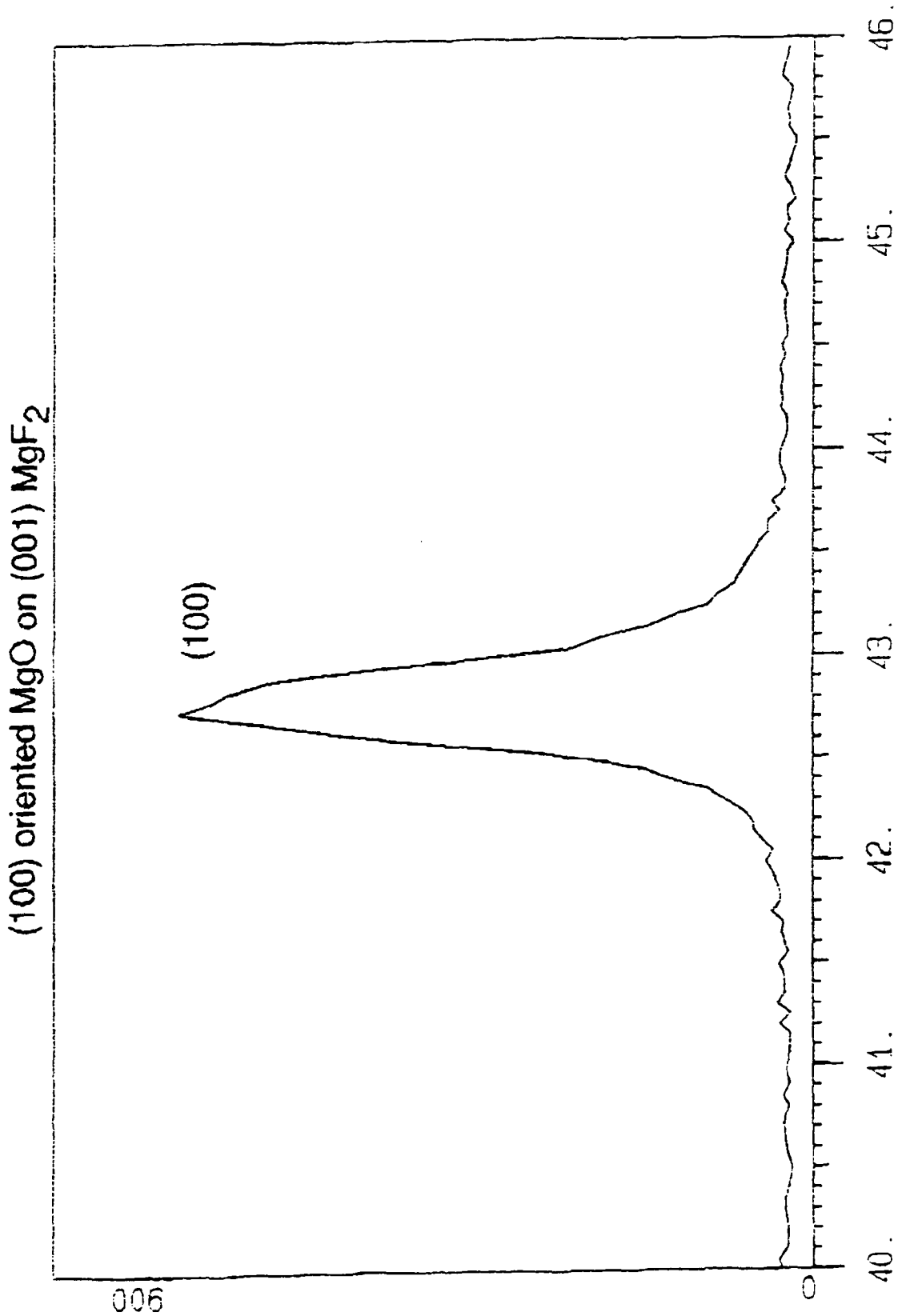

Fig. 1. X-ray fraction profile of an MgO buffer layer.

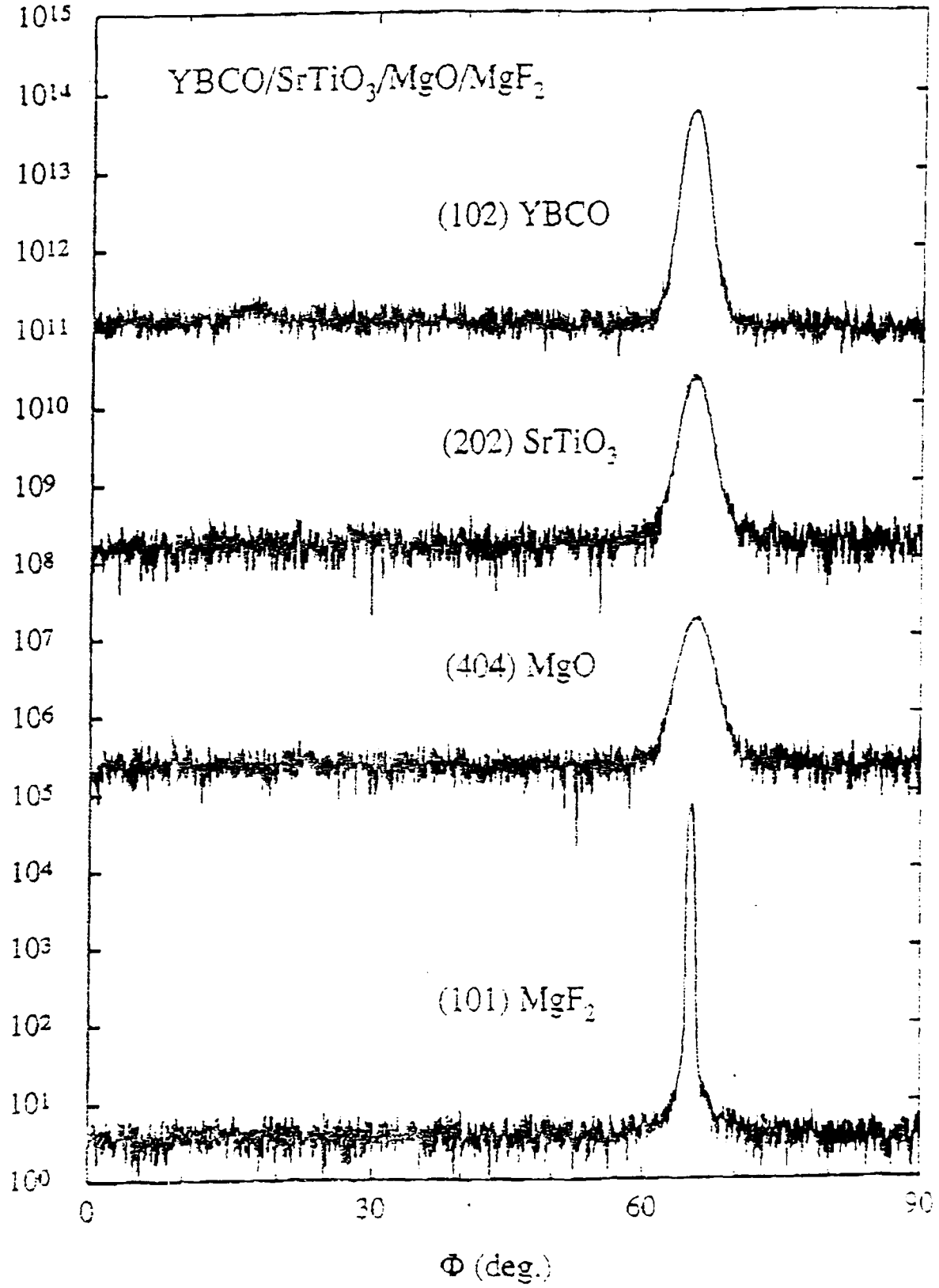

Fig. 2. X ray pole figure data (φ scans) of the substrate - buffer layer- YBCO film combination.

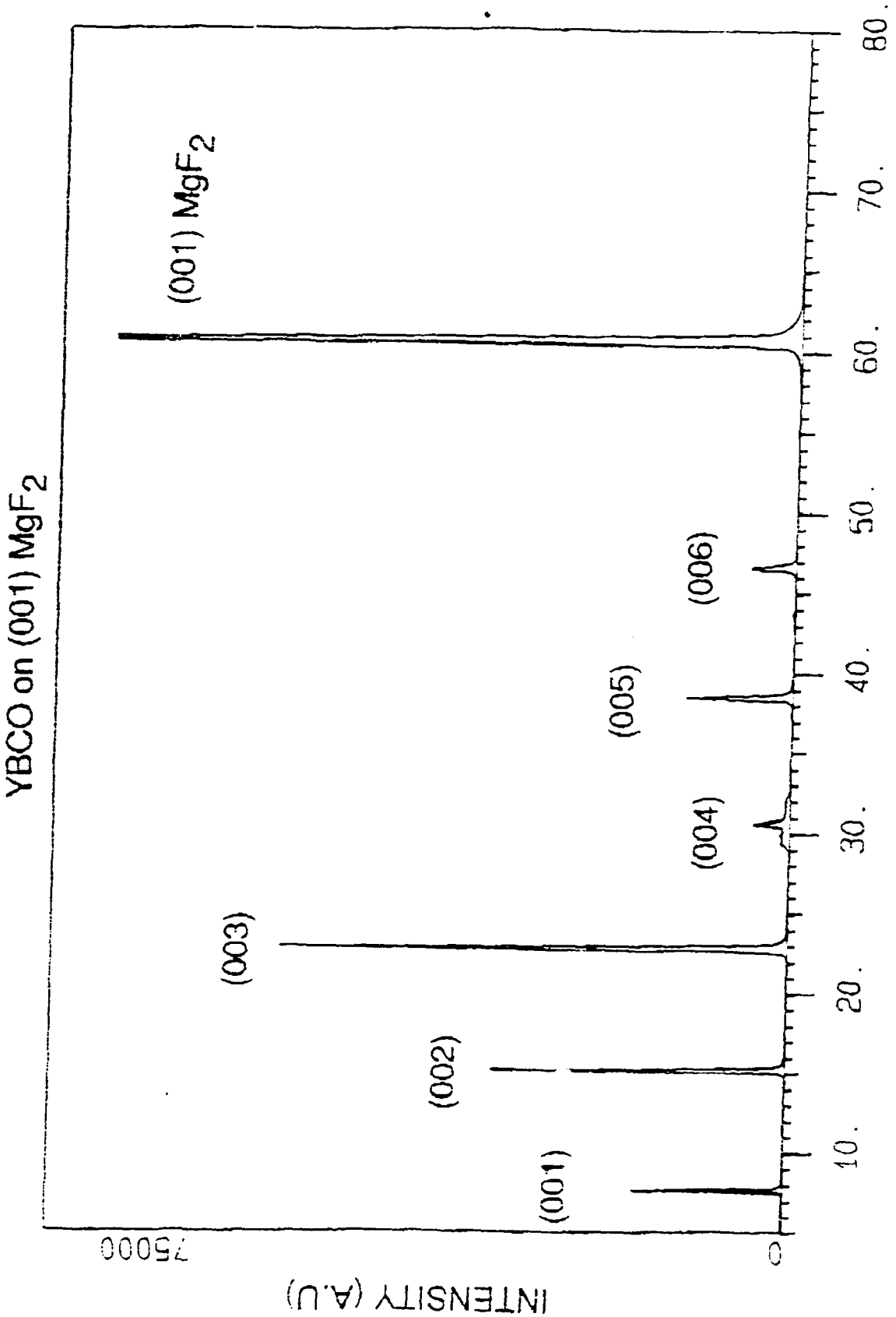

Fig. 3. X-ray - 2ϕ data of the substrate - buffer - YBCO film combination.

The superconducting properties of the films are measured by ac susceptibility and Figs. 4 and 5 represent typical data obtained on the films. The films routinely exhibit T_c's of 88-89K with transition widths ~ 0.5K. The dc resistivity of the films as a function of temperature is shown in Fig. 6. The T_c's suggested by these plots are in the 90 K range with transition widths less than 1K. It may be mentioned here that the T_c zero in the dc resistivity plots corresponds approximately to the T_c onsets in the corresponding ac susceptibility plots. The resistivity of the normal state extrapolates linearly through the origin as observed in the case of high quality YBCO films. The J_c of the films is measured by the 1 μV/mm criterion and is $4x10^6$ A/cm^2 at 77K in zero field. These T_c's and the J_c values are among the highest reported for YBCO films grown on fluoride substrates until now.

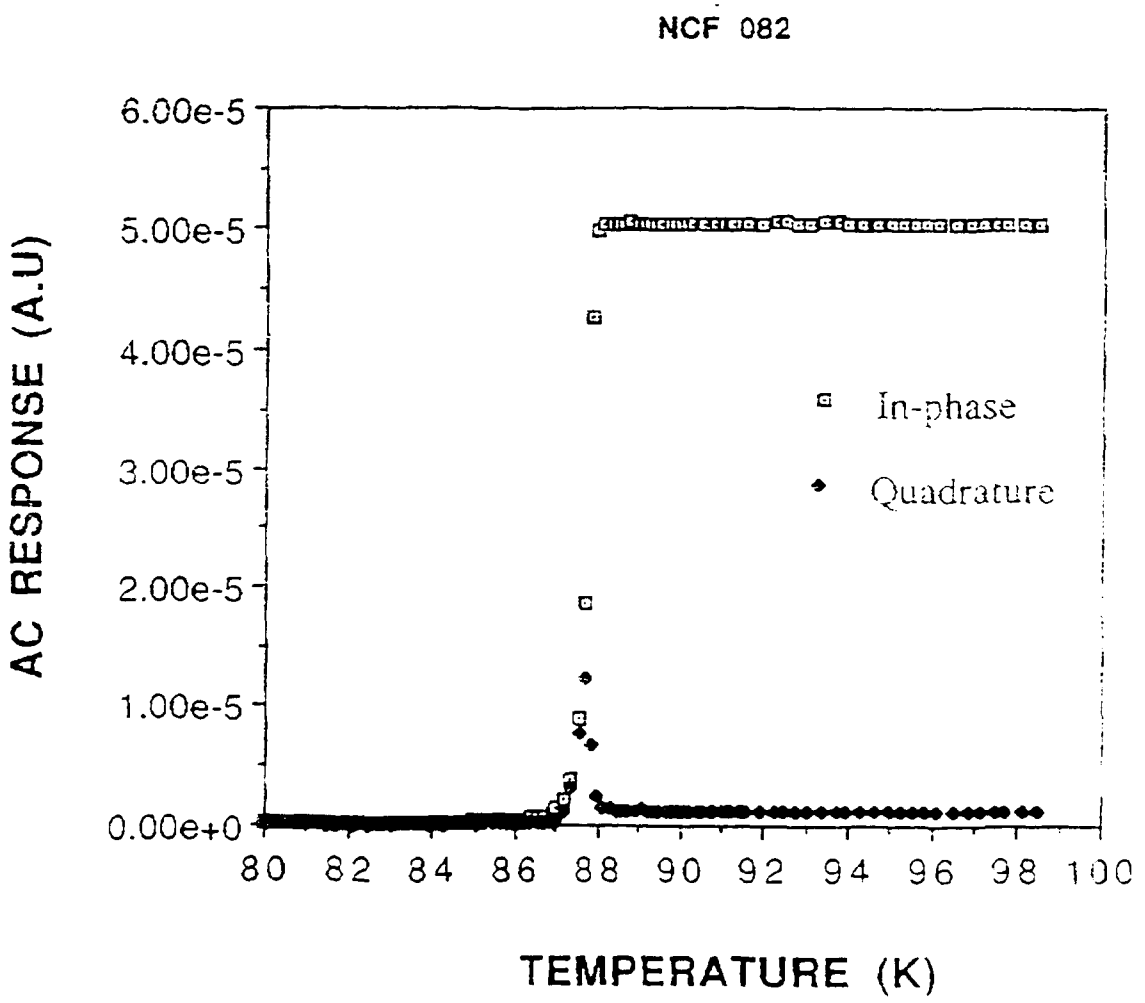

Fig. 4. AC susceptibility data for YBCO on MgF_2 (Sample NCF 082).

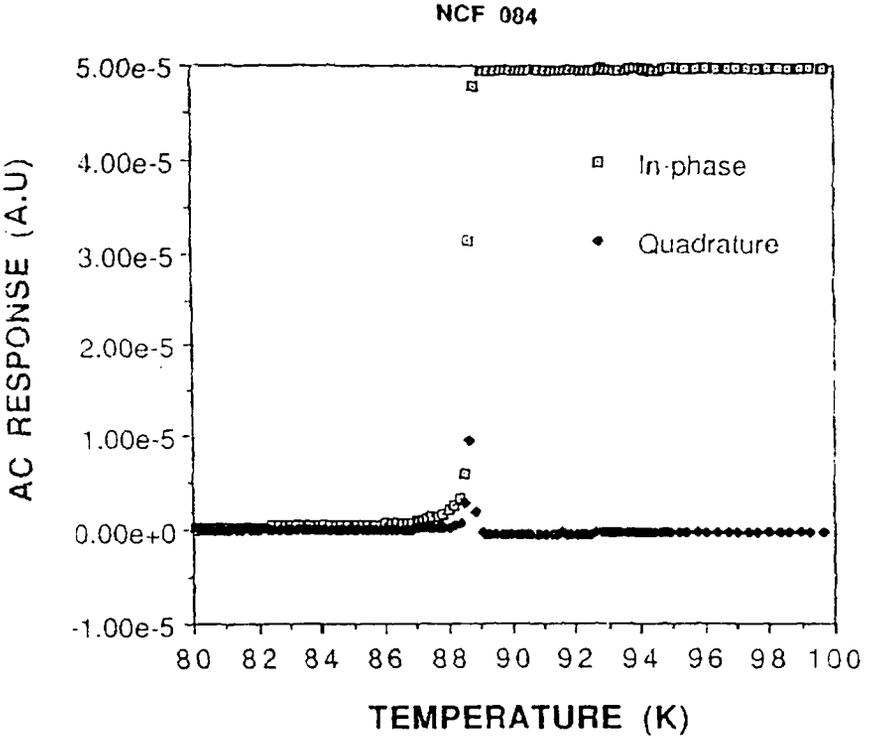

Fig. 5. AC susceptibility data for YBCO on MgF_2 (Sample NCF 084).

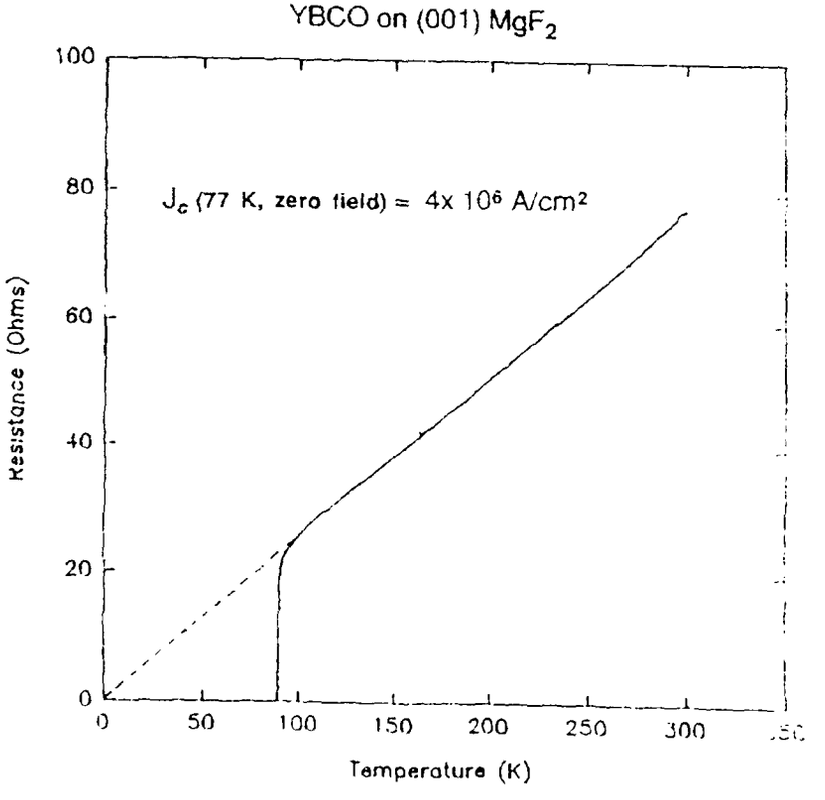

Fig. 6. DC resistivity of the YBCO films versus temperature.

II. SUPERCONDUCTOR SAMPLE CHARACTERIZATION

A. HTS Film Characterization

1. Unpatterned HTSC Films

a. Measurement Results

During the past quarter, we received four $MgF_2/MgO/SrTiO_3/YBCO$ samples from Neocera, which are summarized in TABLE 1. Each sample was 1 cm x 1 cm, with a 1000Å MgO buffer layer, 100Å $SrTiO_3$ buffer layer, and 3000Å YBCO layer. The transition temperatures, T_c, was 88K for sample NC210109 and 89K for the rest of the samples. The transition width, ΔT, was 0.5K for all four samples. The surface quality of these films was similar, each had 5μm pinholes.

Samples NCF075 and NCF076 were measured using the dielectric resonator test set at 77K and 24 GHz. The results for both samples were very encouraging, Q_0 = 27,000 for NCF075 and Q_0 = 29,000 for NCF076. The figure showing Q_0 versus temperature is shown in Figure 7. It shows a comparison with the Q_0 for an HTS film on a lanthanum aluminate substrate (sample NC203046).

Table II. YBCO/MgF_2 SAMPLES

No.	Sample No.	Tc midpt (K)	Tc width (K)	Surface	Size (cm)	Meanderline* Q0	Dielectric Resonator Q0†	Filter Design	Status
1	NCFO75	89.00	0.50	fair	1x1	-	27000	-	
2	NCFO76	89.00	0.50	fair	1x1	-	29000	-	
3	NC210108	89.00	0.50	fair	1x1	-	-	-	
4	NC210109	88.00	0.50	fair	1x1	1085	-	-	meanderline

***Q0 measured at 10 GHz, 77K**

†Q0 measured at 24 GHz, 77K

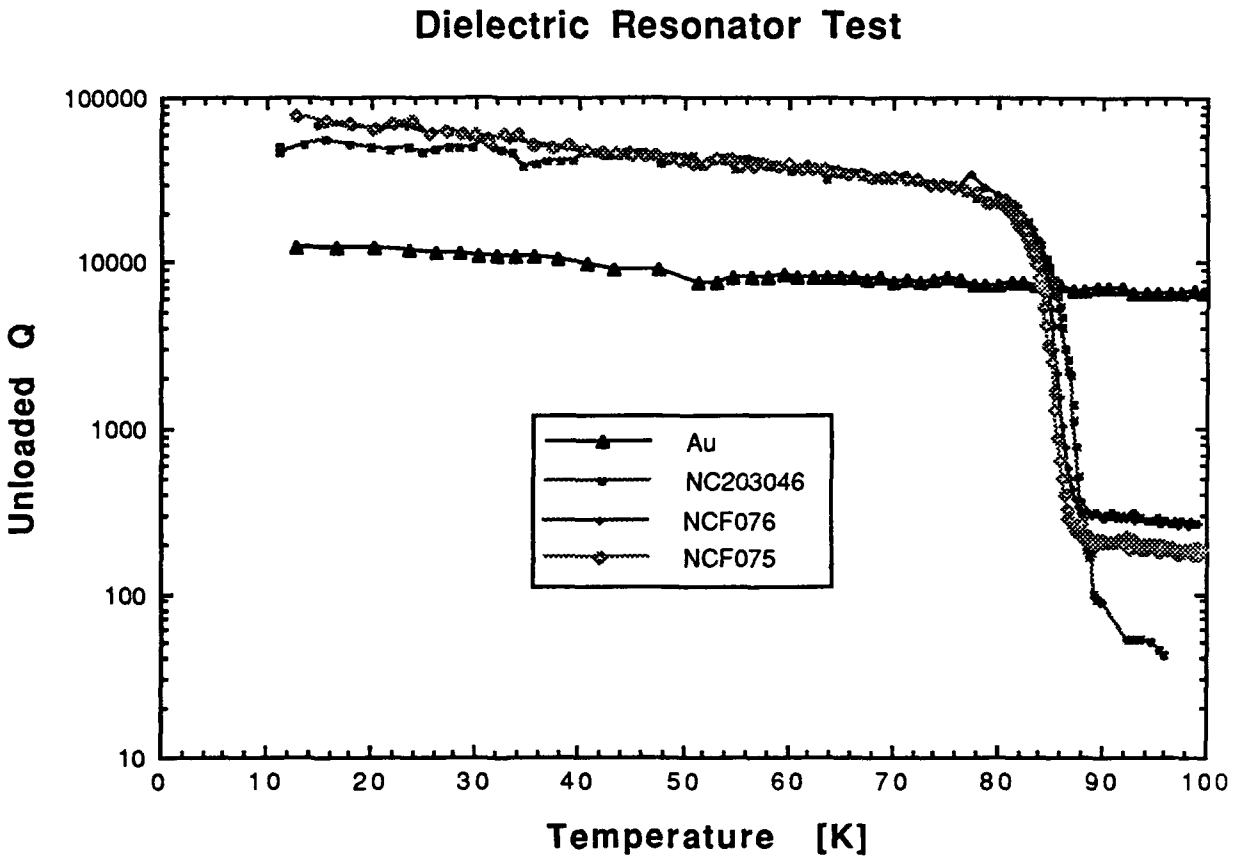

Fig. 7. Unloaded Q vs. temperature with two samples of HTS films on MgF_2 (NCFO76 and NCFO75) in comparison with Au and with a previous HTS film on $LaAl_2O_3$ (sample NC203046).

b. Calibration refinement of dielectric resonator test system

We have successfully measured the conductivity of pure copper ground plates and the loss tangent of the BMT dielectric resonator material at room temperature. We used one sample, and then two samples of the same dimensions stacked one on top of the other to determine these values. These calibration numbers are needed to refine our measurement setup calibration. Currently the numbers we use for making surface resistance measurements of HTS films are published data for the BMT material and the calculated gold-plated brass conductivity from equation (2) of the first Quarterly Status Report [4].

The measurements for one and two samples at room temperature are given by:

One sample:

f_0 (GHz)	Q_0	Diam	Height	ε_r
25.0742	2471	3.63 mm	1.61 mm	24.5

Two stacked samples:

f_0 (GHz)	Q_0	Diam[1]	Diam[2]	Height[1]	Height[2]	ε_r
25.0284	4053	3.62 mm	3.63 mm	1.61 mm	1.61 mm	24.5

Based on these measurements and using Eq. 3 of the first Quarterly Status Report [4], we have calculated the loss tangent of the BMT material and the conductivity of the copper plate at room temperature. The BMT loss tangent is = 0.88×10^{-4} which is very close to the published results of the manufacturer of $Q_d = \frac{1}{\tan \delta} = 10^4$ at 24 GHz. The conductivity of the copper plate is 5.64×10^7 s/m, which is very close to its theoretical value. These reported results are extremely repeatable and based on an average of six measured samples.

Further measurements at 77K are still needed with the single and two stacked samples to finalize this calibration refinement process.

c. Three-axis positioning system

Cryo industries is fabricating the three axis positioning system for the dielectrometer test system. At present, most of the components are complete. The linear cross slides which control the sample holder arm are due shortly from the manufacturer. When they are received, final integration and test will begin. Some of the parts needed had long lead times and consequently delayed this portion of the effort.

2. Patterned Films

a. Processing of HTS film

A meanderline circuit was fabricated on sample NC210109 which resulted in a Q_0 = 1085 at 10 GHz and 77K. This result, which is comparable to YBCO films on sapphire, points to MgF_2 as a promising substrate material. The 25μm wide meanderline was processed using standard fabrication techniques. The YBCO film is coated with positive photoresist and the meanderline pattern is exposed

and developed. The unwanted YBCO is removed by ion beam milling. Finally, the photoresist is removed.

Although the meanderline circuit did not require Au contacts, future circuits fabricated under this contract, such as filters or couplers, will require them. A preliminary investigation into improving the current contact fabrication method was started. At present, a modified lift-off technique is employed. After the YBCO is patterned, photoresist is applied and the contact area is opened up. An 8000Å gold seed layer is sputtered over the photoresist. Without removing the photoresist or gold layer, an additional coating of photoresist is applied and the contact area is then plated up to approximately 5μm with additional gold. The top layer of photoresist is removed in acetone. The seed layer of gold is subsequently removed by ion beam milling and the first layer of resist is removed by acetone. This method offers relatively thick contacts which are suitable for bonding of wires or ribbons. Although we find this method to be successful, a reduction in the fabrication time would improve efficiency and thus save money.

The current modified liftoff method is employed because of difficulties encountered in lifting off thick layers of metal. Recent advances in polyimide coatings have produced polyimide release layers suitable for lift off. Our goal is to apply the polyimide release layer, define it with photoresist, deposit a thick gold layer and remove the unwanted gold and polyimide release layer in one step. This would eliminate the second photoresist layer and the gold plating.

PiRL III from Brewer Scientific was chosen as the polyimide release layer. It can be applied with a spinner and patterned using positive photoresist and positive developer. A release agent from Brewer Scientific or any other strong base can be used to strip or liftoff the PiRL III. Unfortunately, the PiRL III develops isotropically which results in a significant undercut. The PiRL III would typically overdevelop by up to 12μm on each side of the 25μm and 50μm test pattern squares. Variations in the developer concentration, from 3:1 (water:developer) to 6:1 did not reduce the undercutting, nor did increasing the critical prebake times or temperature for the PiRL.

Although our initial efforts to modify the contact fabrication process have not been successful, the importance of contacts for HTSC circuits warrants future efforts in this area.

b. Meanderline Resonator Results

The meander line resonator test system, used extensively for surface resistance measurement, was calibrated with a copper meander line on a 0.5 mm MgF_2 substrate. The measured results for the copper sample indicate Q values of 51.9 and 104 at 2.5 and 10 GHz, respectively.

Sample NC210109 is a YBCO film on 0.5 mm MgF_2 with suitable buffer layers. The Q measurements for this line are shown below in Fig. 8. The measured results for the YBCO sample indicate Q values of 686 and 1085 at 2.5 and 10 GHz respectively. This indicates a minimum improvement of an order of magnitude in surface resistance at 10 GHz and 77K. The roll-off in measured Q at low frequencies has been observed on other HTS samples where local defects in the meander line lower the Q factor.

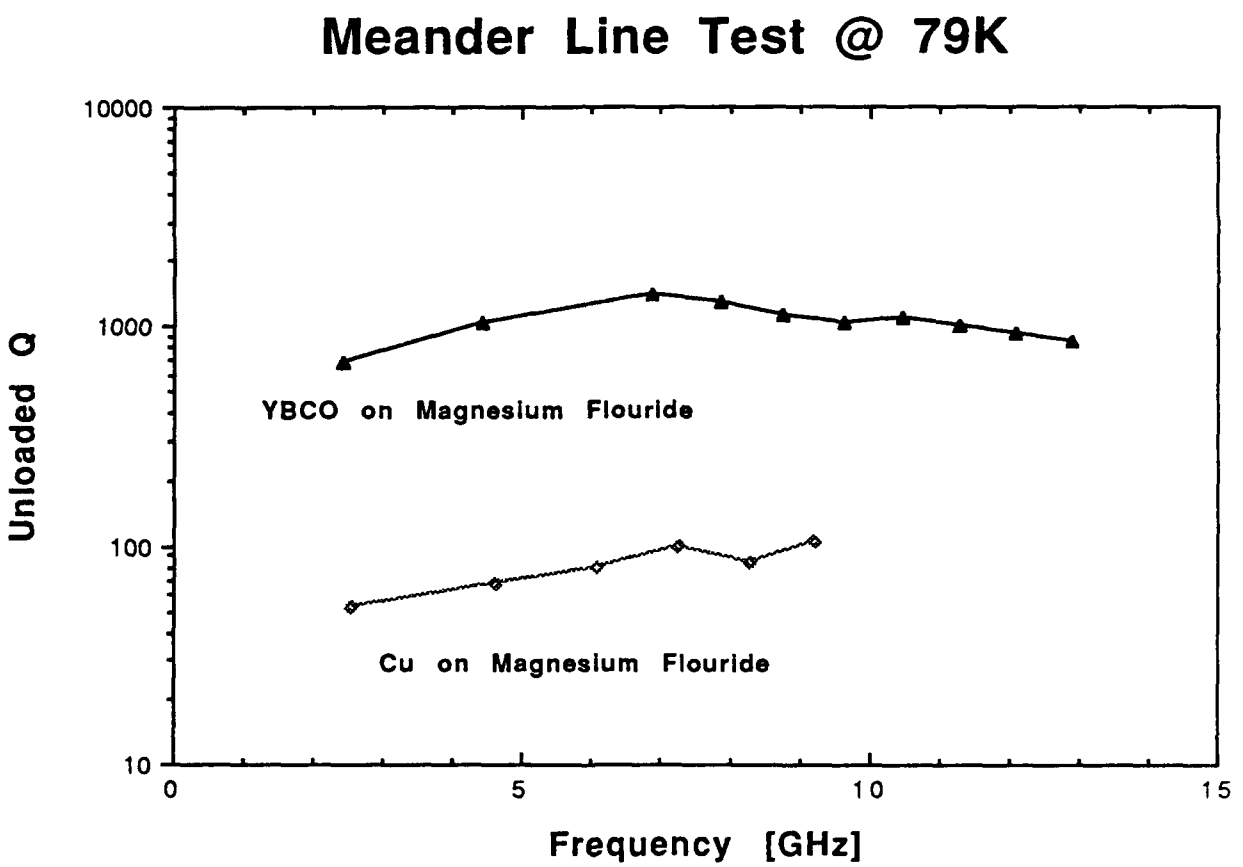

Fig. 8. Meander line resonator Q versus frequency for YBCO on MgF_2 in comparison to copper.

B. Substrate Characterization

1. Calibration at 77K

We are continuing efforts to verify calibration of the dielectrometer at low temperatures. Measurements were performed on a Cordierite sample manufactured by TransTech. The dielectrometer software supplied by Kent Laboratories calculates the dielectric constant and loss tangent from the measured Q data.

The manual supplied with the dielectrometer states "The loss tangent calculation requires subtraction of cavity losses from total losses. When both numbers are small, but comparable, an accurate difference is not possible. Since cavity losses are not well known, only upper and lower bounds are calculated. The difference, which is a measure of resolution, increases with frequency." The plots of loss tangent in Fig. 9 show two lines indicating the "upper and lower bounds," produced by the software. Fig. 10 gives a plot of the Cordierite's dielectric constant versus temperature. Cordierite is a good candidate for a substrate material to be used with the HTS film lift-off technique mentioned in the last quarterly report [5]. It has a low dielectric constant (4.3) and a reasonably low loss tangent of 3×10^{-4} at 77°K.

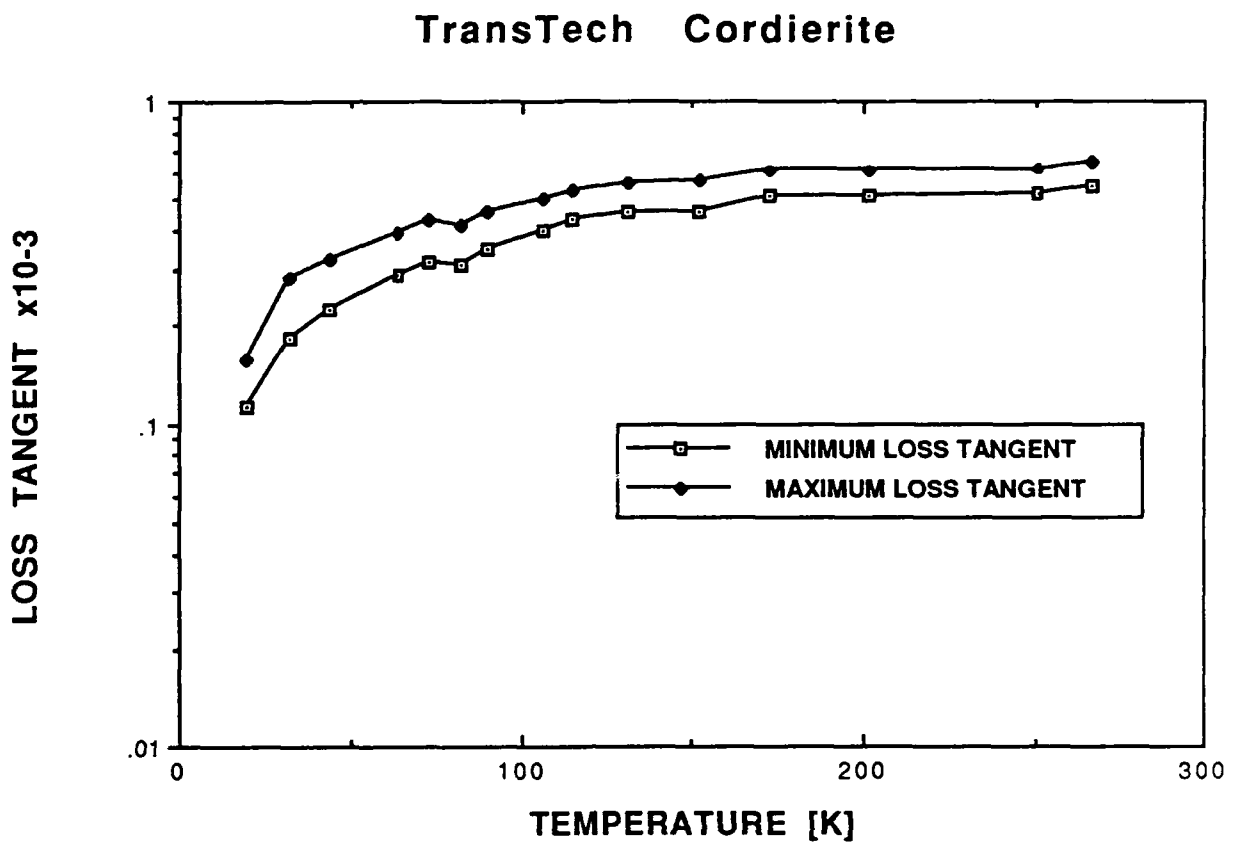

Fig. 9. The loss tangent of cordierite (supplied by TransTech) vs. temperature using the dielectrometer technique.

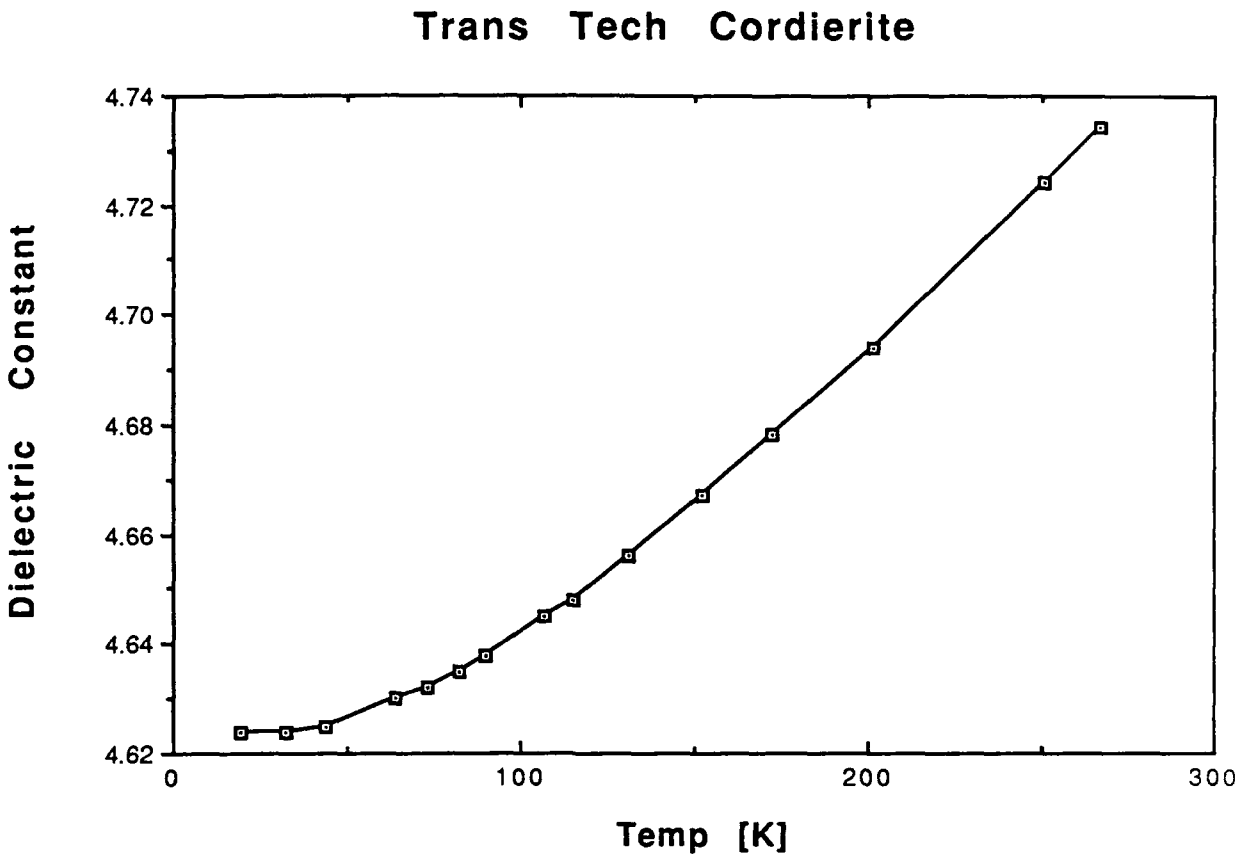

Fig. 10. Dielectric constant of cordierite vs. temperature using the dielectrometer technique.

2. Characterization of Magnesium Fluoride

A Magnesium Fluoride sample was also measured by the dielectrometer technique. Plots of loss tangent and dielectric constant versus temperature are shown in Figs. 11 and 12. At 77K the loss tangent has a good low value of about $1x10^{-4}$ while the dielectric constant exhibits a minimum of about 5.32. Note that the electric fields of the dielectrometer waveguide cavity are oriented in the plane of the thin MgF_2 substrate, which is perpendicular to the crystal's c-axis. The value of dielectric constant that we measured checks closely with the value supplied by the crystal source given in section I.A. From these measurements we can conclude that magnesium fluoride appears to be an excellent substrate for use at microwave and mm-wave frequencies.

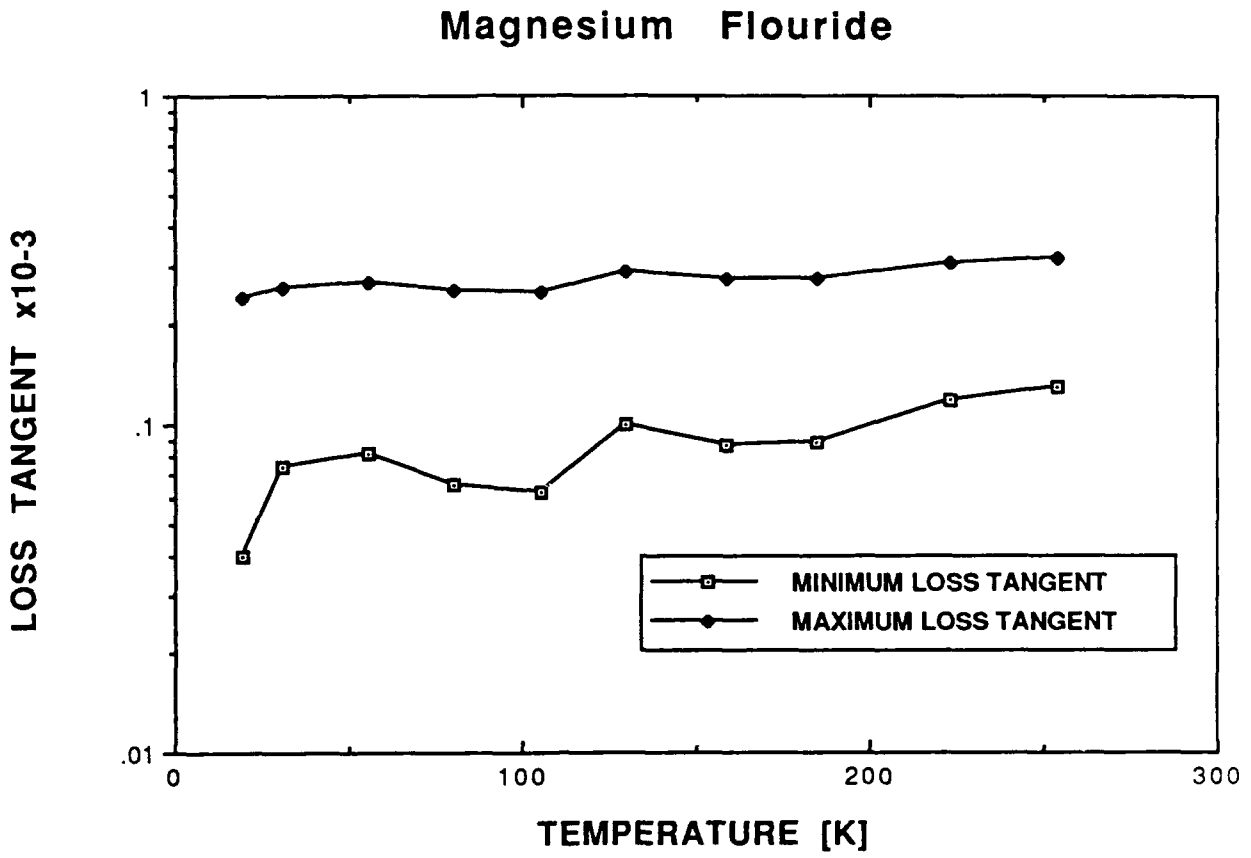

Fig. 11. Dielectric loss tangent vs temperature for a Magnesium Fluoride substrate using the dielectrometer.

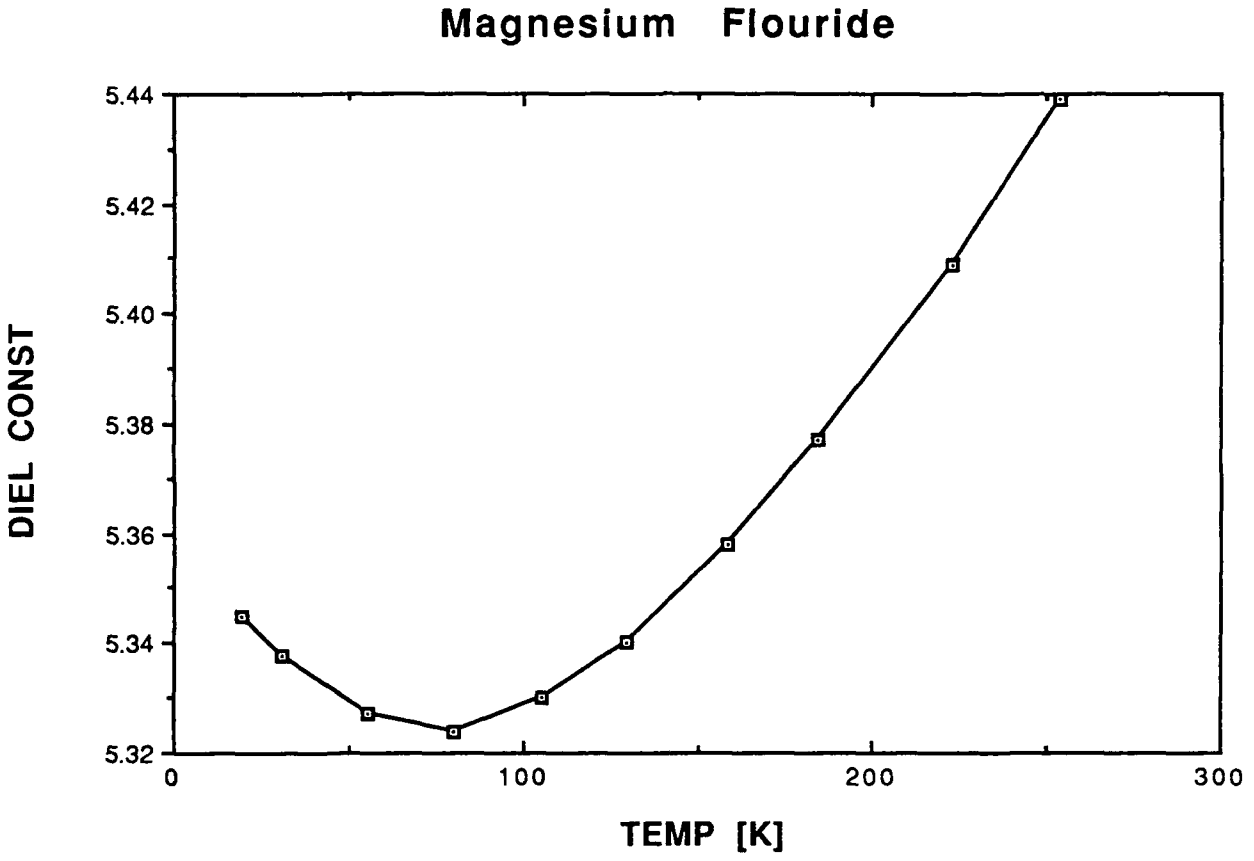

Fig. 12. Dielectric constant vs. temperature for magnesium fluoride using the dielectrometer.

III. Modelling of HTS/Substrate Structure

A. Effect of Buffer Layers and HTS Film Metallization

For a practical application, Neocera suggested a two buffer layer structure for the superconducting material deposition on a low ε_r Magnesium Fluoride substrate ($\varepsilon_r = 5$). The first buffer layer is MgO with $\varepsilon_r = 9.5$ (at 77K), and the second layer is YSZ with $\varepsilon_r = 40$ (at 77K). Neocera routinely deposits layers with a thickness of about 1000Å. With these inputs we conducted a study of the dielectric loss value as a function of microstrip line strip width. These calculations were carried out with substrate heights of 1016, 635, and 254 μm and at frequencies 0.1, 1, and 10 GHz, respectively, as indicated previously in the last Quarterly Status Report [5]. The effect was most significant for narrow lines, thinner substrates, and higher frequencies. At 10 GHz, for example, the dielectric losses of 0.1 cm width lines are roughly 2X higher than those lines with a width of 0.5 cm. These dielectric loss values are still lower than the copper conductor losses, but for superconductor lines with one to two orders of magnitude improvement in conductor loss, the dielectric losses are comparable to conductor losses, especially for narrow lines.

We have extended this study to include the effect of various microstrip metallization schemes on the conductor losses for different line widths. A 254μm thick substrate with a dielectric constant of 5 was assumed. Table III summarizes the results at both 10 GHz and 35 GHz which were obtained by using a commercially available program called PCAAMT [6] for analysis of multi-layer dielectric and conductor structures. Significant improvement in loss is evident if an all-superconducting material is used. The use of a superconducting strip and a normal ground plane will show moderate improvement which could be enough for early development stages.

Table III.
Effect of Various Microstrip Metallization Schemes on Loss

At 10 GHz:

	Cu both sides	HTS top metal Cu Ground plane	HTS both sides
W = 254 μm (ε_{eff} = 3.55, Z_o = 71 Ω)			
conductor loss (dB/cm)	0.0419	0.0134	0.0042
dielectric loss (dB/cm)	0.0018	0.0018	0.0018
W = 508 μm (ε_{eff} = 3.77, Z_o = 49 Ω)			
conductor loss (dB/cm)	0.0379	0.016	0.0038
dielectric loss (dB/cm)	0.0016	0.0016	0.0016
W = 762 μm (ε_{eff} = 3.94, Z_o = 37 Ω)			
conductor loss (dB/cm)	0.0384	0.0181	0.0038
dielectric loss (dB/cm)	0.00178	0.00178	0.00178

At 35 GHz:

W = 254 μm (ε_{eff} = 3.58, Z_o = 72 Ω)	All Cu	Top HTS	All HTS
conductor loss (dB/cm)	0.0800	0.0286	0.0080
dielectric loss (dB/cm)	0.0066	0.0066	0.0066

IV. SAMPLE CIRCUIT DESIGN

A. General mm-Wave Circuit Design Considerations

Conventional millimeter wave circuits use dielectric substrates of relatively low dielectric constant such as fused quartz (ε = 3.8) to suppress propagating modes other than the fundamental quasi-TEM mode. With larger ε, thinner substrates are required. For example, both MgO and sapphire have a dielectric constant of about 10 and require a substrate thickness of less than 125 μm for millimeter wave circuits operating up to 60 GHz. The other popular HTS

substrate, $LaAlO_3$, has a dielectric constant of 25, which makes it virtually impractical at such frequencies. MgF_2 substrates are excellent for these applications with its low dielectric constant of approximately 5 since the use of this dielectric allows for practical mode-free performance using a substrate thickness of about 250 μm.

Only single-sided HTS coated substrates are currently available from Neocera. There is the possibility of realizing an HTS ground plane by placing a single-sided HTS patterned circuit on top of another HTS-coated substrate serving as ground. However, this approach is not likely to yield results close to design because of inevitable airgaps between the two substrates which will have significant effects at mm-wave frequencies. Therefore, the use of a double-side coated substrate is preferable for the final filter realization and will be available from Neocera in the near future. For the initial design and experimental verification, readily available single-coated substrates are satisfactory. The following describes the design of two sample circuit types, a narrowband filter suitable for multiplexers and a power divider that is a key component for array antenna feed networks.

B. Filter Design

From the classic filter design equations, the insertion loss in dB at midband of a coupled resonator filter (L_o) is approximately given by

$$L_o = 4.34 \frac{f_o}{\Delta f} \sum_{k=1}^{n} \frac{g_k}{Q_{uk}} \quad \text{in dB} \tag{1}$$

Here, n is the number of poles, g_k are the normalized series inductances and shunt capacitances values of the low pass prototype filter, Q_{uk} is the unloaded quality factor for the k-th resonator, and Δf is the filter's bandwidth. Assuming a Chebyshev 4-pole filter with 0.01 dB equal amplitude ripple and the use of identical resonators, equation (1) becomes:

$$L_o = 21.6 \frac{f_o}{\Delta f\, Q_u} \quad \text{in dB} \tag{2}$$

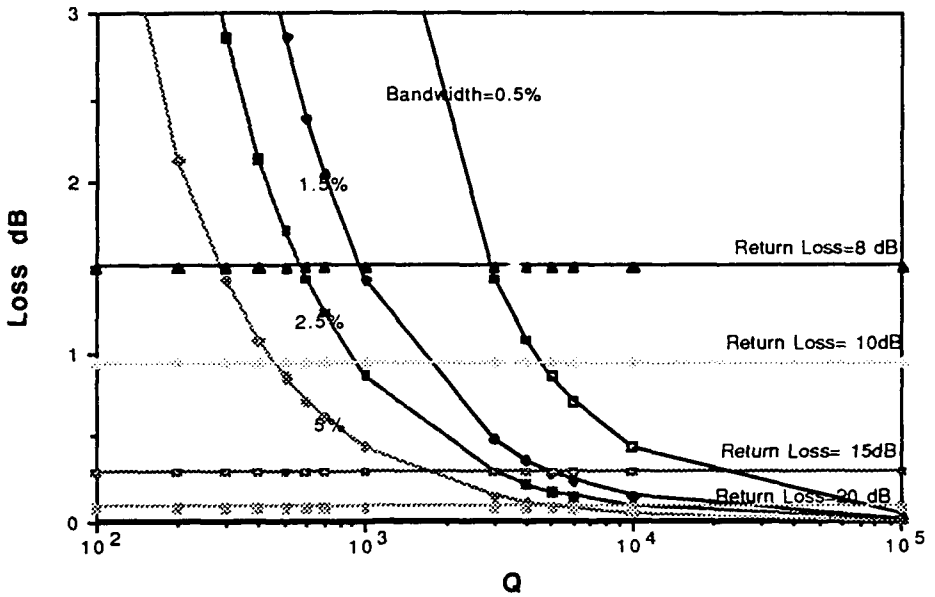

Fig. 13. Midband insertion loss versus required resonator unloaded Q for a four-pole Chebyshev filter.

Based on the above equation, Fig. 13 shows the effect of resonator Q and bandwidth on the midband insertion. For example, $Q = 2 \times 10^4$ will produce 0.3dB insertion loss and 15dB return loss for a BW of 0.5%. Assuming we can achieve a surface resistance for an HTS film that is 10X better than copper at 35 GHz, the use of the computer program for calculating microstrip loss predicts a 3X improvement in filter loss with only an HTS center strip (normal Au ground plane) and by another factor of 3X by using a double-sided HTS circuit.

Due to accuracy limitations in most circuit models, available CAD programs do not yield an acceptable synthesis for most filter structures when the dielectric constants of the substrates are greater than 18. A few percent error in the dielectric constant will lead to a substantial center frequency deviation. However, we have found a good combination of analytical tools (CAD programs Midas [7], Smith [8], and Parfil [9]) suitable for both analysis and design of microstrip line filters. Parfil has proven to give correct strip width and spacing values, but its predicted resonator lengths have been inaccurate. Our in-house

simulation program MIDAS has been helpful in modifying the design for improved accuracy.

For an NRL HTS multiplexer program [10], we have designed, built, and tested 4-pole microstrip line X-band filters on a lanthanum aluminate substrate. Designs using Parfil with 35 Ω internal impedances were utilized. Room temperature insertion loss measured 12.8 dB without tuning, and the superconducting version with a copper ground plane gave a midband insertion loss of 1.7 dB after using some tuning screws. Midas was extensively used to analyze the measured response and a modified version showed an insertion loss of 1.3 dB at 77K with no tuning. These filters had a Au ground plane. An insertion loss of 0.6dB is expected for an all-HTS filter.

Based on this experience with HTS filters at X-band, we have designed 4-pole and 6-pole bandpass microstrip filters operating at mm-wave frequencies. These filters have a narrow bandwidth of 100 MHz to demonstrate the superior performance of HTS over copper at 35 GHz, and have Chebyshev characteristics with 20dB return loss and a 0.01 dB in-band ripple. It is extremely advantageous from the design point of view to work with low ε_r substrates since CAD software for microstrip lines on low dielectric constant substrates is readily available for filter designs. A double-sided HTS coated MgF_2 substrate will be used when available from Neocera. Initially, single-sided HTS coatings along with a gold ground plane will be fabricated.

The chosen filter configurations are shown in Figs. 14 and 15. The major features of the filter design with the double-sided HTS coating are:

- Minimal ground plane losses.
- Compact circuit size of about 1.2 cm x 1.2 cm.
- Wider lines for better power handling capability
- Wider lines for lower sensitivity to pin holes.
- Ease of tuning with low loss dielectric slugs (if necessary).

B. Power Divider for a mm-Wave Feed Network

To demonstrate the superior performance of HTS films at 35 GHz, our initial proposal included a sample circuit component that could be applied to a planar feed network for phased array antenna applications. Waveguide feeds, although relatively low loss, are very heavy, bulky, and difficult to integrate with other components. Regular microstrip or suspended substrate feed networks are very compact but too lossy to be used at millimeter wave frequencies with

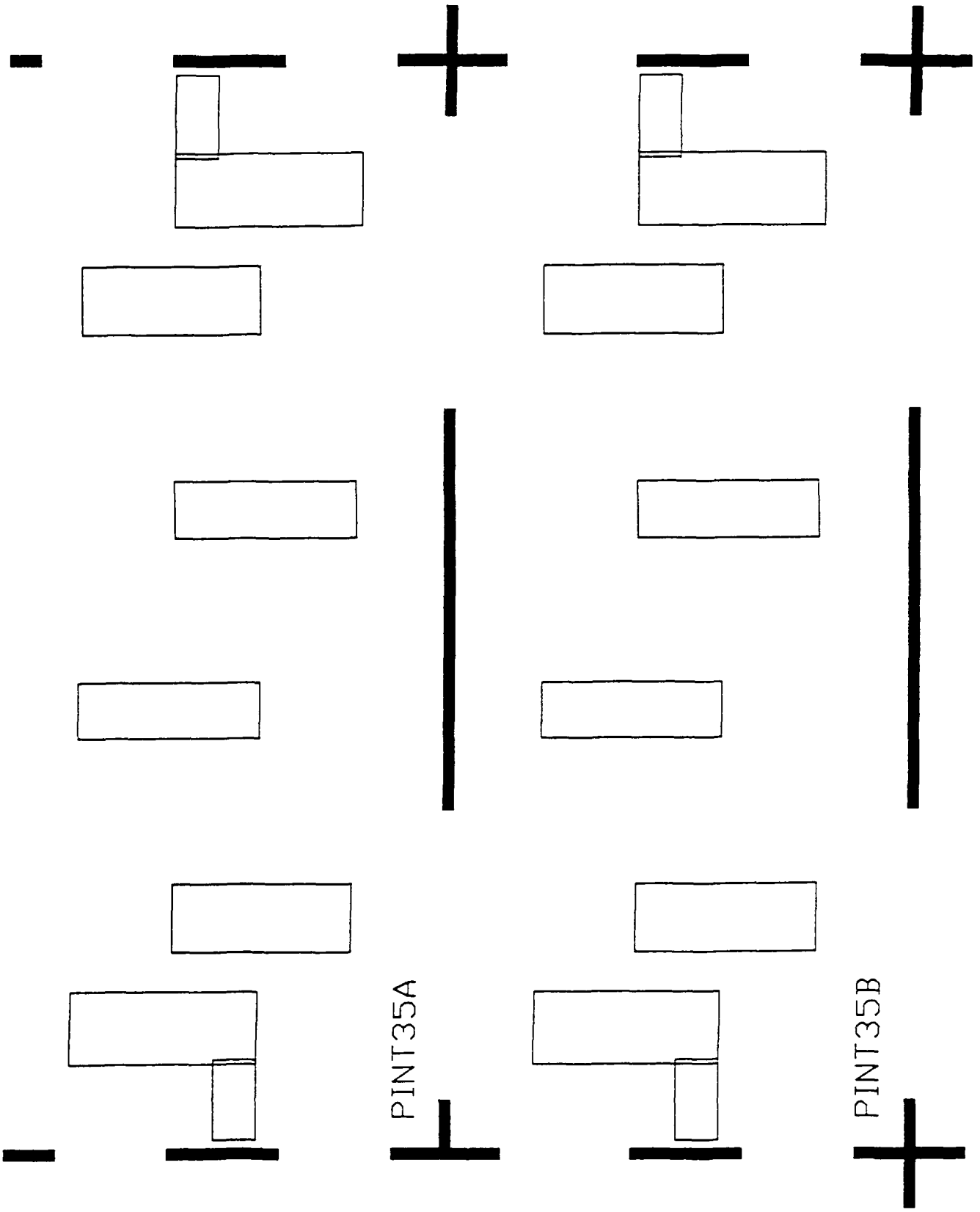

Fig. 14. Interdigitated 35 GHz Filter

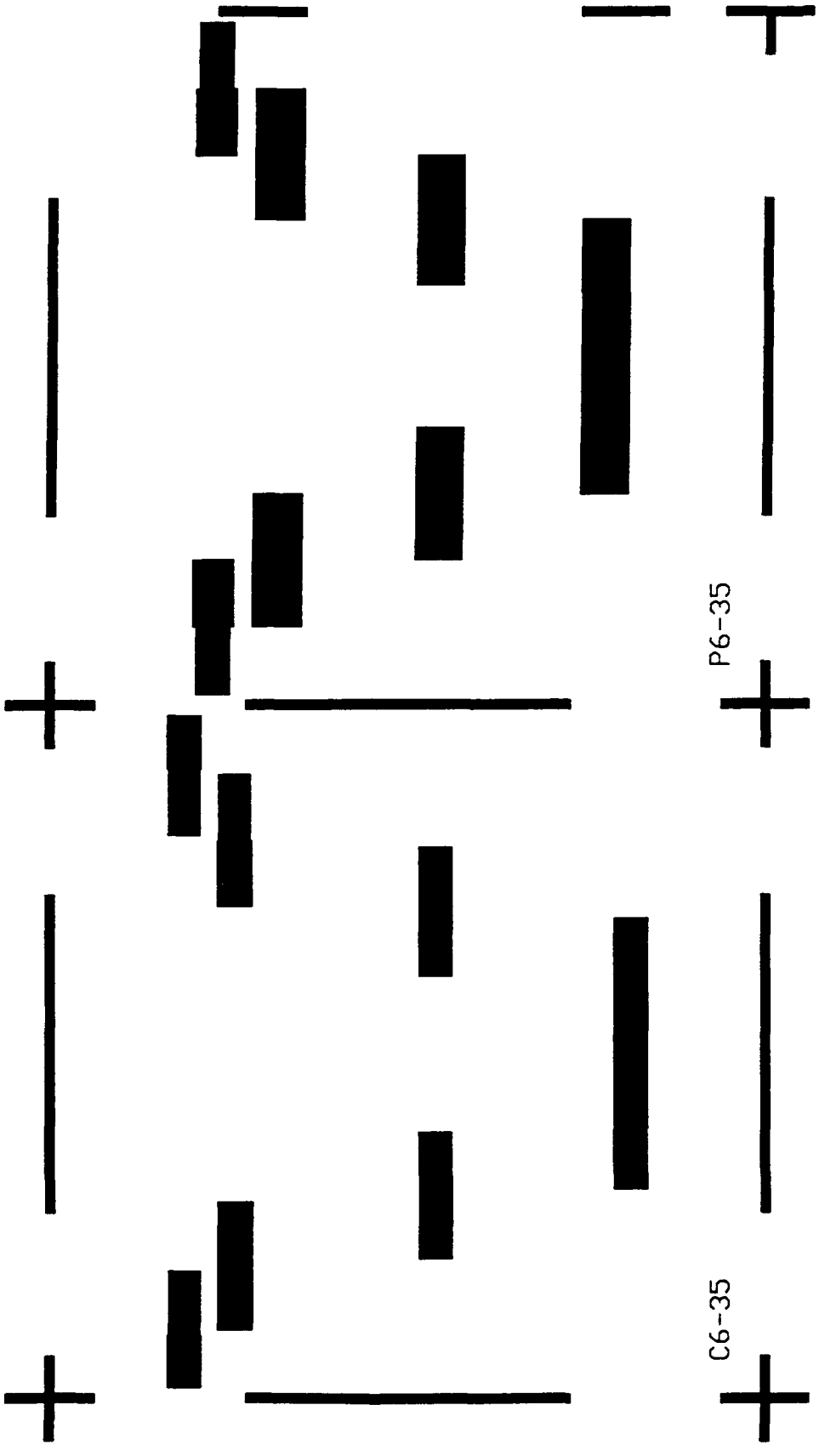

Fig. 15. Coupled Line 35 GHz Filter

conventional metallization. The use of a high quality HTS film on a low dielectric constant substrate like MgF_2 will enable us to realize low loss, light weight feed networks for millimeter wave antenna arrays.

The feed network can be either a suspended substrate or a microstrip configuration. However, for integration with other components and to insure the highest degree of compactness, microstrip is the preferred approach. By keeping the dielectric constant low, the losses at 35 GHz can be made even smaller than that of a waveguide. For example, using a 250μm thick substrate with a dielectric constant of 5, the loss of a 50 ohm transmission line becomes 0.77 dB/m (where the surface resistance of the HTS film is assumed an order of magnitude higher than copper at 77K and 35 GHz); for comparison, a standard copper waveguide line has 1dB/m loss.

A key component of the feed network chosen for a sample circuit is a modified Wilkinson 3 dB power splitter shown in Fig. 16. This configuration permits the use of grounded termination resistors instead of a co-planar balance resistor used in a conventional Wilkinson divider. A loss of 0.1 dB for the HTS version is expected as compared to 0.4 dB for the copper version. Copper circuits will initially be fabricated and tested as a reference. HTS circuits will follow.

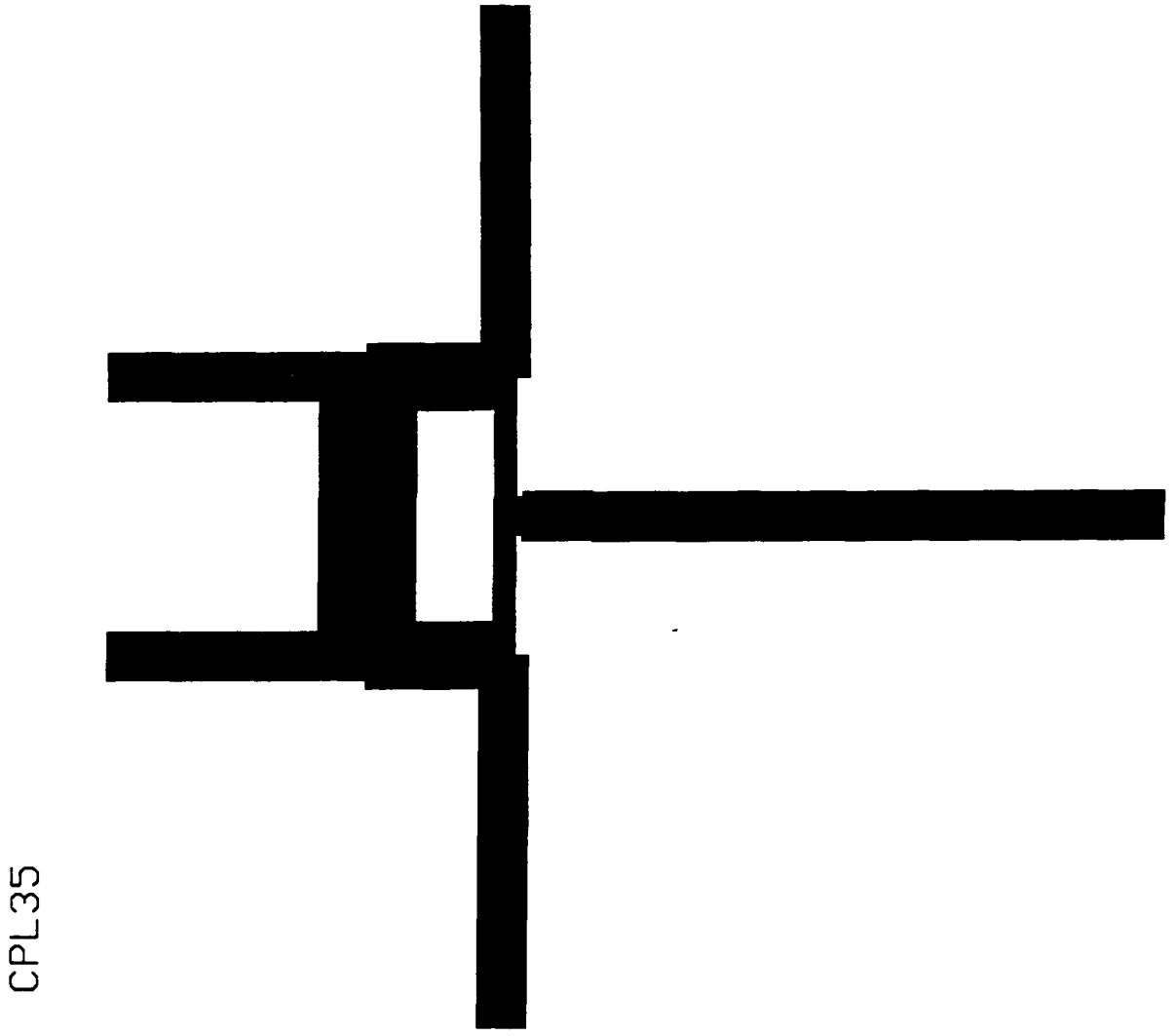

Fig. 16. Modified Wilkinson Power Divider

V. REFERENCES

1. S. Yadavalli et al., Phys. Rev **B1**, 7961 (1991).
2. I. S. Gergis et al., Appl. Phys. Lett. **60**, 2026 (1992).
3. R. Ramesh et al., Appl. Phys. Lett. **56**, 2243 (1990).
4. R&D Status Report No. 1 for period 9/24/91 to 1/31/92.
5. R&D Status Report No. 3 for period 5/1/92 to 7/31/92.
3. PCAAMT, Linear analysis of planar transmission lines Package, D. Pozar, Antenna Design Associates, Leverett, MA.
7. Midas, Linear Circuit Analysis program, S. Perlow, David Sarnoff Research Center, Princeton, NJ.
8. I. John Smith," The even and odd mode capacitance parameters for coupled lines in suspended substrate," IEEE MTT Trans., Vol. MTT-19, No. 5, May 1971, pp. 424-431.
9. Parfil, Analysis and design of coupled line filter structures, K. Johnson, Southwest Microsystems, Escondido, CA.
10. D. Kalokitis et al., "High temperature superconducting x-band multiplexer," Interim report for NRL, Oct 1992.

VI. CHANGE IN KEY PERSONNEL: None

VII. SUMMARY OF SUBSTANTIVE INFORMATION DERIVED FROM SPECIAL EVENTS: None

VIII. PROBLEMS ENCOUNTERED AND/OR ANTICIPATED: None

IX. ACTION REQUIRED BY THE GOVERNMENT:

Approval for transfer subcontractor

X. Fiscal Status

1. Amount currently provided on contract: $550K
2. Expenditures and commitments to date: $466K
3. Funds required to complete work: $1,585,085